Quantum Computing with Charge States in Silicon : Towards a Leadless Approach

Thierry Ferrus, Alessandro Rossi, Aleksey Andreev, Paul Chapman and David Arfon Williams
Hitachi Cambridge Laboratory, J J Thomson avenue, CB3 0HE, Cambridge, United Kingdom
Email: taf25@cam.ac.uk

***Abstract*—Coherence time and the ease of operability of a device are well-known requirements for the realization of individual qubits. However, the successful integration of many devices further restricts the choices for implementation. In this article, we describe a device in which manufacturing considerations have been taken into account for the device design and the choice for material, and where leadless control of the qubit is possible.**

***Keywords*-Quantum computing, silicon, charge qubit, quantum dots**

I. INTRODUCTION

Since the early development of integrated circuits in 1958, the continuous decrease in transistor size, as described by Moore's law [1], has been driven by the continued demand for increasing computing power. This has been mainly facilitated by technological advances, which allow the incorporation of a progressively large number of smaller transistors onto a single chip. Quantum mechanical effects have been found to be increasingly important in the behavior of conventional devices at the nanometer scale, and this has led to substantial research into the quantum properties of nanoscale objects. In addition, devices on this scale offer the possibility of making circuits for quantum information processing and quantum computing, a notion first suggested by Feymann [2].

In the past decades, many architectures have been proposed as platforms for quantum computation [3] most using an optical or a solid-state approach. All make use of quantum bits or qubits, an analogue of the classical bit, as an essential element of computation. Some of these realizations have been particularly successful, such as superconductor-based qubits with Josephson junctions, trapped ions or coherent photon states. This is primarily due to the choice of the material, the ability to perform fast measurements as well as the simplicity of the system. However, a practical implementation for circuit applications requires high fidelity results, a good scalability, and preferably a high compatibility with existing manufacturing techniques. This has driven several proposals attempting to use silicon as the basis for qubit realization, because of its compatibility with current fabrication methods. (An example is the well-known Kane proposal for quantum computation [4]) Silicon has intrinsic properties such as potentially the absence of intrinsic nuclear spins, which make it a desirable choice for qubit as well as conventional transistor fabrication. In semiconductor approaches, we can broadly define two qubit types: Charge qubits, where the basis states are defined by two distinct electron distributions, and spin qubits where the representation is in the spin orientation of electron or nucleus.

In this article, we first review the technological and commercial constraints that led to our choice for employing charge qubits in an isolated silicon structure, with an emphasis on flexibility, reliability, cost and compatibility with conventional fabrication techniques. We then define the qubit states for that specific system and describe how basic quantum operations could be performed under DC voltages, in particular the initialization stage and swap operations. Supported by recent and ongoing experimental investigations, we finally show that specific device features could be used for future leadless operation of the system that would ultimately simplify scalability.

II. TECHNOLOGICAL CHOICES

Some materials that have been considered for the manufacture of qubits, such as III-V compounds, possess apparently significant advantages, in particular a direct band gap and the possibility to reduce interface scattering through layer design [5]. However, issues such as the finite nuclear spin, leading to spin qubit decoherence, and strong dipole scattering from polar phonons, decohering charge qubits, make silicon still appear a material of choice for manufacturing future qubit processors.

Another important consideration for future commercialization is the need for high reproducibility, both in the device fabrication and in quantum operation readouts. Devices must have a high fabrication yield and their electronic characteristics or behaviors must be consistently reproducible. There are several pathways to realize a solid state qubit. One of the more recent consists in using the spin state of a localized electron at a donor site in silicon [6], [7], as was suggested by Kane [4]. Although easily allowing both charge and spin qubit manipulation, this concept is difficult to scale because of the requirement for precise single ion positioning and the inherent donor diffusion during anneal stages. Another option in silicon is the use of quantum dots with dimensions of a few tens of nanometers. For such a structure, a singly charged quantum dot pair or double quantum dot is appropriate. Because the dimensions lie within the range of transistor sizes that are currently

 ISBN: 978-1-61208-151-9

manufactured, the industrial infrastructure is already well adapted to this future technology.

In order to realize any type of solid-state qubit, one has to minimize sources of noise to keep a coherence time sufficiently long and be able to perform a significant number of operations before re-initialization of the qubit becomes necessary. Unfortunately, and despite line filtering and careful contact designs, high frequency noise can reach the device via highly conducting paths such as gate or source and drain leads. In addition, it is desirable to minimize the number of leads to ease the process fabrication, especially for 3D integration purposes as well as minimizing possible interference effects. From this perspective, ungated devices seem preferable, and these will be described here.

These devices consist of a double-dot charge qubit, where the quantum states $\mid 0\rangle$ and $\mid 1\rangle$ are represented by two different electron distributions between the lobes of the device, coupled with a detector to measure the changes in charge distribution.

In many solid-state approaches to quantum computation, single electron transistors (SETs) have been the primary choice for detection of charge movement at the fractional charge level. Their design relies on the presence of two tunnel barriers of conductance $\ll e^2/h$ separated by a confined region made of a single dot. Their operation principle is based on Coulomb blockade (CB) resulting in electrons being blocked for transport if the electrostatic configuration is not energetically favourable for tunneling. Tunnel barriers can be controlled by forming metal gates on top of the structure or by patterning constrictions in the device and thus modifying the potential barrier height between the contact and the quantum dot. In both cases, the dot potential has to be controlled by an additional gate. The method described here provides the advantage of physically decoupling the detector from its control gate by allowing a side-gate to be patterned laterally and by etching the unnecessary material between the gate and the dot.

One potential difficulty to be overcome in using doped silicon results from the potential noise in the device itself due to tunneling or hopping events of electrons in the vicinity of the device. In particular, random telegraph signals are detrimental to the measured signal quality, most especially at low temperatures due to electron hops between donor sites. However, such electron dynamics may be controlled by adjusting the doping density, varying the electrostatic field inside the structure [8] or manipulating the trap population by microwave measurement [9]. Following the previous discussions, the use of a doped silicon SET with constrictions and a sidegate then seems a reasonable choice for a qubit state detector.

The noise reduction implementations in the structure can be carried out further by etching the material around the qubit structure, so that direct electron transfer between the qubit and the detector becomes prohibited. Although

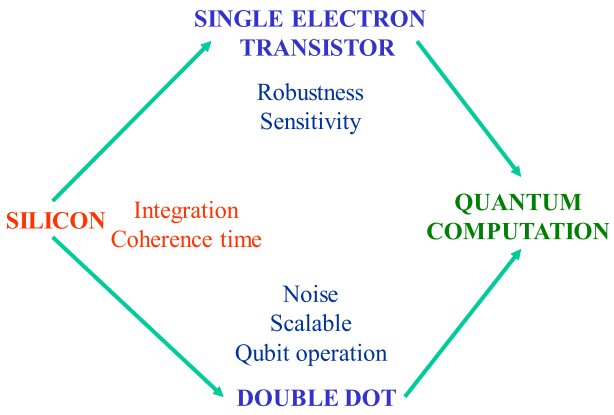

Figure 1. Industrial choices for qubit structures.

necessary in order to obtain longer coherence times, this choice makes measurement more challenging because it is not possible directly to probe the states of the qubit, for example, by using source and drain contacts.

In the next sections, we describe the operation of an isolated double quantum dot (IDQD) structure and present some specific electronic properties. In particular, we show that strong detection of the qubit states could be obtained using a SET (Figure 1) and that leadless qubit operation using microwaves is conceivable.

III. Principles and DC qubit operation

A. *Qubit definition and initialization*

Owing to the doping concentration, the size, and the geometry of the dots, usual simulations based on capacitance calculations are insufficient fully to describe the transport characteristics of the device [8]. Indeed, the operation of the qubit is strongly influenced by the presence of localized states at the edge of the structure and electron-electron interaction within and between dots. As a consequence, electron tunneling between dopant states may induce a charge reorganization in the structure. The understanding of the electronic properties of an IDQD capacitively coupled to an SET then requires the use of multi-electron physics in simulations.

To this end, the qubit states have to be defined as an effective charge excess in one of the two IDQD dots. An effective charge is defined by the variation in the electrostatic potential that would be created by a single-electron tunneling event in a metallic structure. This takes into account the possibility for the electron to tunnel between donor sites in the same dot as well as charge rearrangement. The initial electron population in each dot, N_1 and N_2, is initially defined by the range of gate voltages used to operate the device. We then have :

 ISBN: 978-1-61208-151-9

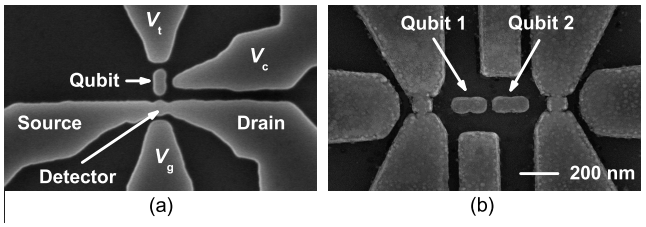

Figure 2. a) Single qubit device and its detector. Control gate are V_g for the SET and V_c and V_t for the IDQD. b) Fabricated two qubit devices with two SET detectors in the same configuration

$$|\,0\rangle = |\,N_1, N_2\rangle \tag{1a}$$

$$|\,1\rangle = |\,N_1+\delta, N_2-\delta\rangle \text{ with } N_1+N_2=N \tag{1b}$$

Here, N is the total number of electrons in the IDQD, excluding localized electrons at the Si-SiO_2 interface and δ the effective charge displaced. N is fixed at the etching stage in the process.

Within the proposed geometry, a single qubit structure required two gates to be patterned. One close to SET and one close to the IDQD. Due to capacitance coupling between the gates, the SET and the IDQD, compensation techniques [10] have to be implemented in order to maintain the detector in the most sensitive region during qubit operations. Such a structure design allows high scalability to ungated multi-qubits (Figure 2b). However, for a single qubit test structure, it is possible to use a third detuning gate in order to avoid compensating voltages [8] (Figure 2a).

The initial states $|\,0\rangle$ and $|\,1\rangle$ are defined by mapping the SET current with the SET gate and the IDQD gate V_c. The presence of a significant shift in the CB peak position defines the set of gate voltages (V_{g0}, V_{c0}) and (V_{g1}, V_{c1}) for which the two states could be accessed. The magnitude of the Coulomb peak displacement in gate voltage is dependent on the tunnel barrier between the two IDQD dots but also on the relative coupling strength between the SET and the two IDQD dots. The efficiency in the charge detection is then enhanced if the IDQD is oriented perpendicular to the source drain leads of the SET because of the produced difference of sensitivity and capacitance between the SET and the respective upper and lower IDQD dot. This configuration was chosen to this end.

In the case of uncompensated operations, the gate voltages are fixed at the degeneracy region where the two states are in superposition of states (V_g^*, V_c^*) and the third gate defines the $|\,0\rangle$ and $|\,1\rangle$ states (V_{t0}^*, V_{t1}^*) (Figure 3).

B. Quantum logic operations

Quantum logic operations are usually performed by a set of pulses sent via the side-gate leads and describing simple unitary operations. Such a technique has been successfully

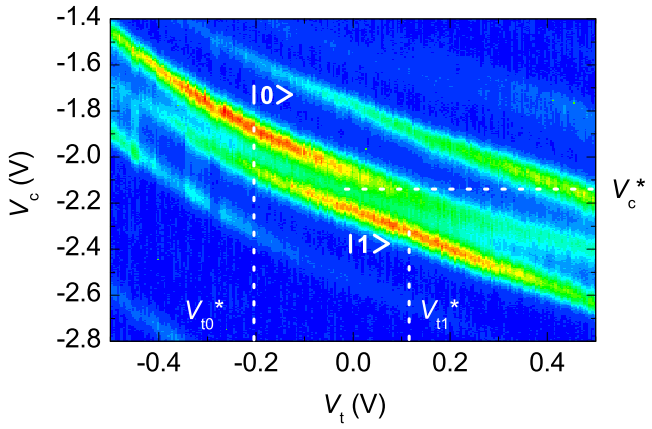

Figure 3. Operation points for the qubit with $|\,0\rangle$ and $|\,0\rangle$ states. Colors map the dependence of the SET current I_{SD} on gate voltages, with high (low) current values in red (blue).

applied in a SET coupled IDQD structure and Rabi oscillations have been demonstrated [11]. Due to capacitance coupling between the different elements of the nanostructure, including the qubit, the detector and the various gates, reliable operations require the use of gate compensation technique, synchronous triggering of the gate signals and well-controlled pulse transmission in high frequency lines.

As an alternative method to trigger and control the displacement of electrons between the two IDQD dots, in the next section we describe an experimental approach to control a qubit using centimeter-waves with leadless coupling.

IV. Leadless operation and scaling

Radio and microwave signals can be coupled to the device either directly, via gates, or in a leadless approach by broadcasting them using an antenna (electrical coupling) or a coil (magnetic coupling) [12]. For the latter, the coupling is weaker but efficient matching can be obtained even at low temperature. In previous experiments, the control signal $h\nu$ was set to be in resonance with the energy difference between two neighboring phosphorous sites in the SET [9]. In most cases, the operating frequency was in the gigahertz (GHz) range and electrons were able to be displaced between the two sites. This was possible although $h\nu \ll kT$ because of the poor electron-phonon coupling in these structures [13]. Such a microwave-induced electron displacement can be coherent, and control of the Rabi rate can be achieved, as demonstrated in similar devices [14]. In these experiments, the resonant condition was determined by a sharp increase in the SET current due to a modification of the tunneling barrier profile. Because the SET and the IDQD are made of the same material, it is conceivable that specific frequencies may address localized electrons at the phosphorous sites in the IDQD. Although some electron hops in the IDQD will not be detected by the SET due to their location,

 ISBN: 978-1-61208-151-9

away from the detector, some can induce a sufficiently large effective charge displacement so that the SET could detect them. This possibility is supported by the observation of the effect of random telegraph signals (RTS) on the electron population in the IDQD dots in some devices. RTS result from random jumps of electrons between donor sites and are generally considered as a source of electronic noise at low temperature. If present in devices, they result in abrupt shifts in the CB peak positions in gate voltage in single electron transistors.

However, there is a difference depending on such events take place in the SET or in the IDQD. For the former, the charge occupancy in the dot is abruptly modified and leads to a shift in all CB peak positions in gate voltage by a same amount and independently of the IDQD configuration. However, RTS in the IDQD mostly affect the SET at the degeneracy region. Due the dot electrical insulation, RTS in the IDQD can only be probed indirectly by assessing their influence on the SET conductivity.

When the qubit is set in the superposition of state $\mid 0\rangle\cos(\phi) + \mid 1\rangle\sin(\phi)$, RTS induces a phase shift close to $\pi/2$, leading to a partial electron population inversion in the IDQD (Figures 4 and 5). Because RTS operate in the same way as previous microwave controlled electron tunneling, this observation enlighten the possibility to control the qubit for specific microwave frequencies. Such an experimental test was carried out by coupling microwave to the device in a leadless approach that resolves the problem of impedance matching, both in a region of qubit operability and outside for comparison. At a frequency of 7.5775 GHz, we observe that the normal SET operation is not affected by the microwave for any power whereas a partial population inversion was realized when the qubit is tuned in its operating point and the power of the microwave close to 0 dBm (Figure 6). For this configuration we did not observe any heating effect due to the microwave absorption nor increase in the electron temperature. These results thus demonstrate that a suitable frequency and power level could lead to a controlled population inversion in the qubit and so to a phase shift.

Because the value of the frequency operating the qubit is depending on both geometrical constraints and the quantum dot internal structure, it is possible to modify or adjust the frequency during the process of the device, so that different frequencies could be associated to different qubits. This is technologically advantageous for scalability purposes because the difficulty in addressing various qubits is reduced to the implementation of frequency multiplexing. This idea was partly demonstrated in previous experiments [15].

V. Conclusion

We have presented a possible implementation of a solid-state qubit that is compatible with current commercial fabrication techniques and with a potentially long decoherence time due to its isolated nature. Despite geometrical constraints, a successful and large detection signal was obtained and the qubit basis states were mapped in a gate dependency diagram. We have also shown that this specific implementation can offer the possibility for leadless operation, especially in the microwave range, leading to easier scalability. Finally, the choice for silicon as a base material to realize the qubit offers the advantage of using a similar structure in order to implement spin qubits.

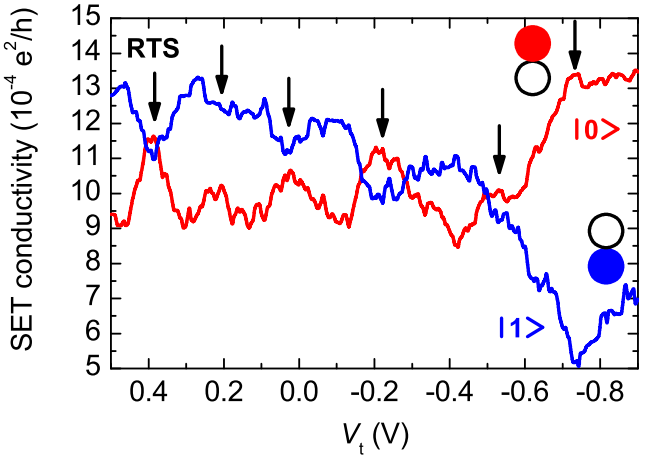

Figure 4. SET current profiles along V_t for the two qubit state configurations. RTS events are present and induce partial population inversions when the qubit is set in an entangled state with $\phi \sim \pi/4$. For $V_t < -0.6$V, states are clearly projected on qubit basis states.

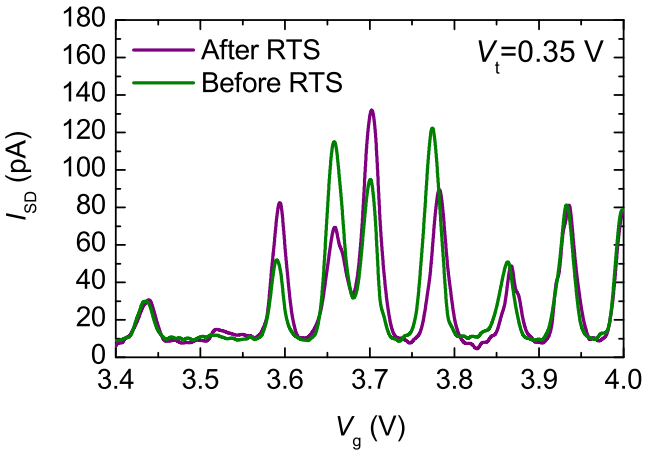

Figure 5. CB oscillations as a function of V_g at a fixed qubit gate voltage V_t. RTS events modify the SET current I_{SD} level around the degeneracy region ($V_g \sim 3.7 \pm 0.1$ V) whereas the other CB peaks remain unaffected.

Acknowledgment

This work was partly supported by Special Coordination Funds for Promoting Science and Technology in Japan.

 ISBN: 978-1-61208-151-9

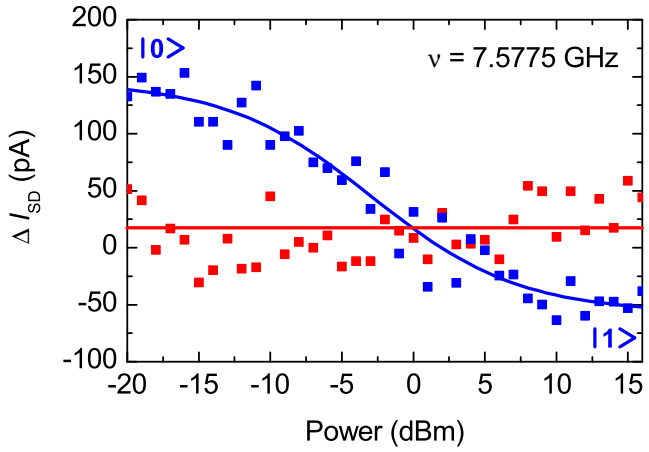

Figure 6. Microwave manipulation of the qubit. ΔI_{SD} is related to the change in the number of electrons in the upper IDQD dot ($|0\rangle$ state). The red trace shows the dependence of the SET current in a region outside the operating point of the qubit whereas the blue trace shows a transition from the $|0\rangle$ to the $|1\rangle$ state.

REFERENCES

[1] G. Moore, *Cramming More Components onto Integrated Circuits*, Electronics Magazine, vol. 38, No. 8, 1965

[2] R. P. Feynman, *Simulating physics with computers*, Int. J. Theor. Phys., vol. 21, pp. 467-488, 1982; *ibid Quantum Mechanical Computers*, Optics News, Vol. 11 Issue 2, pp.11-20, 1985

[3] W. S. Warren, *The Usefulness of NMR Quantum Computing*, Science, vol 277, pp. 1688, 1997; A. Shnirman, G. Schön, and Z. Hermon, *Quantum Manipulations of Small Josephson Junctions*, Phys. Rev. Lett., vol 79, pp. 2371, 1997; A. Steane, *he Ion Trap Quantum Information Processor*, Appl. Phys. B., vol 64, pp. 623, 1997; S. Takeuchi, *Experimental demonstration of a three-qubit quantum computation algorithm using a single photon and linear optics*, Phys. Rev. A, vol 62, pp. 032301, 2000; D. Loss and D. P. DiVincenzo, *Quantum computation with quantum dots*, Phys. Rev. A, vol 57, pp. 120, 1998

[4] B. E. Kane, *A silicon-based nuclear spin quantum computer*, Nature, vol 393, pp 133, 1998

[5] C. C. Dean and M. Pepper, *The transition from two- to one-dimensional electronic transport in narrow silicon accumulation layers*, J. Phys. C: Solid State Phys., vol 15, pp. L1287, 1982

[6] P. T. Greenland, S. A. Lynch, A. F. G. van der Meer, B. N. Murdin, C. R. Pidgeon, B. Redlich, N. Q. Vinh, and G. Aeppli, *Coherent Control of Rydberg States in Silicon*, Nature, vol 465, pp. 1057, 2010

[7] A. Morello, J. J. Pla, F. A. Zwanenburg, K. W. Chan, H. Huebl, M. Mottonen, C. D. Nugroho, C. Yang, J. A. van Donkelaar, A. D. C. Alves, D. N. Jamieson, C. C. Escott, L. C. L. Hollenberg, R. G. Clark, and A. S. Dzurak, *Single-shot readout of an electron spin in silicon*, Nature, vol 467, pp. 687, 2010

[8] T. Ferrus, A. Rossi, M. Tanner, G. Podd, P. Chapman, and D. A. Williams, *Electron dynamics in a non-metallic silicon isolated double quantum dot capacitively coupled to a single electron transistor*, arXiv:0907.2635, 2011

[9] T. Ferrus, D. G. Hasko, Q. R. Morrissey, S. R. Burge, E. J. Freeman, M. J. French, A. Lam, L. Creswell, R. J. Collier, D. A. Williams, and G. A. D. Briggs, *Cryogenic instrumentation for fast current measurement in a silicon single electron transistor*, J. Appl. Phys., vol 106, pp. 033705, 2009

[10] A. Rossi, T. Ferrus, G. J. Podd, and D. A. Williams, *Charge Detection in Phosphorus-doped Silicon Double Quantum Dots*, Appl. Phys. Lett., vol 97, pp. 223506, 2010

[11] J. Gorman, D. G. Hasko, and D. A. Williams, *Charge-Qubit Operation of an Isolated Double Quantum Dot*, Phys. Rev. Lett., vol 95, pp. 090502, 2005

[12] D. G. Hasko, T. Ferrus, Q. R. Morrissey, S. R. Burge, E. J. Freeman, M. J. French, A. Lam, L. Creswell, R. J. Collier, D. A. Williams, and G. A. D. Briggs, *Single shot measurement of a silicon single electron transistor* , Appl. Phys. Lett., vol 93, no 19, pp. 192116, 2008

[13] J. Ogi, T. Ferrus, T. Kodera, Y. Tsuchiya, K. Uchida, D. A. Williams, S. Oda, and H. Mizuta, *Experimental observation of enhanced electron-phonon interaction in suspended Si double quantum dots*, Jpn. J. Appl. Phys., vol 49, pp. 045203, 2010

[14] A. Rossi and D. G. Hasko, *Microwave-assisted transport via localized states in degenerately doped Si single electron transistors*, J. Appl. Phys. 108, 034509, 2010

[15] M. Erfani, D. G. Hasko, A. Rossi, W. S. Cho, and J. Choi, *Microwave driven arbitrary coupling between trapped charge resonances in a silicon single electron transistor*, unpublished, 2011

 ISBN: 978-1-61208-151-9